

Numerical modelling of air flow over complex terrain concerning wind erosion

MINGYUAN DU

National Institute of Agro-Environmental Sciences, 3-1-1 Kannondai, Tsukuba, Ibaraki 3058604, Japan

PEIMING WU

National Space Development Agency of Japan, 1-9-9 Roppongi, Minato-Ku, Tokyo 1060032, Japan

TAICHI MAKI & SHIGETO KAWASHIMA

National Institute of Agro-Environmental Sciences, 3-1-1 Kannondai, Tsukuba, Ibaraki 3058604, Japan

Abstract A numerical model for simulating wind distribution over complex terrain has been developed concerning prevention of wind erosion. The three-dimensional, time-dependent Navier-Stokes equation written in generalized coordinates and the Smagorinsky-type scheme for turbulent parameterization are used in the model. The most desirable setting for placing a windbreak, for preventing wind erosion, may be decided by simulating the wind distribution over real terrain using the model. Two examples are given and the effects of windbreaks on the prevention of wind erosion are discussed. One example is using a 2-m-high windbreak hedge for preventing sand shifting around a barchan sand dune which is 5 m high, 64 m wide and 96 m long. The simulation results show that the best place should be 18–22 m in front of the top of the sand dune. Another example is using terrace construction and a 2-m-high windbreak hedge for reducing wind speed over a 20-m-high idealized hill. The simulation results show that a terrace construction could reduce over 40% of wind speed on the windward side and that a windbreak hedge at the terrace edge could reduce wind speed a further 20–40% on the windward side. However, there would be an overspeeding region appearing at the two side slopes of the hill.

INTRODUCTION

For centuries windbreaks including forests, nets, fences and hedges have been used worldwide for the prevention of wind erosion. The effectiveness of a windbreak may be illustrated by the modification of airflow patterns. Reviews of recent research has been given by Van Eimern *et al.* (1964), McNaughton (1988), Heisler & DeWalle (1988). Recently, we have carried out some work on windbreak effects in arid land (Du & Maki, 1993, 1997; Maki *et al.*, 1995, 1997) and realized that it is necessary to clarify the effects of windbreaks on air flow over complex terrain. As shown by some recent useful numerical simulations (e.g. Wilson, 1985; Wang & Tattle, 1995) and wind tunnel investigations (e.g. Maki, 1982; Judd *et al.*, 1996), it is relatively easy to observe or to estimate the effect of a windbreak when the windbreak is located in a flat or smooth place. However, it is difficult to know the actual effect a windbreak has on the wind and to determine where in a complex to set the windbreak

for the optimum prevention of wind erosion. To our knowledge, there are no theoretical and numerical studies that address air flow near windbreaks over complex terrain, although some work has been done on numerical simulation of wind flow over a sand dune and sand dune movement (e.g. Wippermann & Gross, 1986; Fisher & Galdies, 1988).

In order to clarify the effects of windbreaks and to determine where to set windbreaks for optimum prevention of wind erosion, a simple numerical model to simulate the mean air flow near windbreaks over complex terrain has been developed (Du *et al.*, 1997). This paper presents some numerical simulation results of the effect of a windbreak hedge on wind speed distribution over a barchan sand dune which is 5 m high and 96 m long by erecting windbreaks at different places, and the effects of terrace and windbreak hedge construction on a 20-m-high idealized hill.

MODEL AND SIMULATION DESCRIPTION

Model description

We consider that the windbreak is about 10 m high and that the height variation of complex terrain is less than 100 m so that the effect of the Coriolis force and thermodynamic variation due to topography and the windbreak may be neglected. Only neutral stratification was considered. In order to catch the influence of sudden variations of topography, generalized terrain-following coordinates (ξ , ψ , ζ) were used which are defined as follows. The vertical line ζ is orthogonalized to the ground surface, orthogonal relationships also existed between the vertical coordinate line and other coordinate lines, ξ , ψ . Thus, under the Boussinesq approximation, the three-dimensional, non-hydrostatic, incompressible atmospheric continuity equation and equation of motion in the generalized terrain-following coordinates (ξ , ψ , ζ) may be written as:

$$\frac{\partial(U/J)}{\partial\xi} + \frac{\partial(V/J)}{\partial\psi} + \frac{\partial(W/J)}{\partial\zeta} = 0 \quad (1)$$

$$\begin{aligned} & \frac{\partial(u_i/J)}{\partial t} + \frac{\partial(Uu_i/J)}{\partial\xi} + \frac{\partial(Vu_i/J)}{\partial\psi} + \frac{\partial(Wu_i/J)}{\partial\zeta} = \\ & - \frac{\partial(\xi_i P/J)}{\partial\xi} - \frac{\partial(\psi_i P/J)}{\partial\psi} - \frac{\partial(\zeta_i P/J)}{\partial\zeta} + \frac{\partial[(\xi_x \tau_{i1} + \xi_y \tau_{i2} + \xi_z \tau_{i3})/J]}{\partial\xi} \\ & + \frac{\partial[(\psi_x \tau_{i1} + \psi_y \tau_{i2} + \psi_z \tau_{i3})/J]}{\partial\psi} + \frac{\partial[(\zeta_x \tau_{i1} + \zeta_y \tau_{i2} + \zeta_z \tau_{i3})/J]}{\partial\zeta} \end{aligned} \quad (2)$$

$$(i = 1, 2, 3; u_i = u_1, u_2, u_3 = u, v, w) \text{ while } \xi_i = \frac{\partial\xi}{\partial x}, \frac{\partial\xi}{\partial y}, \frac{\partial\xi}{\partial z} \text{ etc.})$$

where U , V , W are the generalized terrain-following coordinates (ξ , ψ , ζ) component velocities respectively; u , v , w are Cartesian coordinates (x , y , z) component velocities respectively; ξ_x , ξ_y , ξ_z , ψ_x , ψ_y , ψ_z and ζ_x , ζ_y , ζ_z , are differential calculus for

the subscript (x, y, z , e.g. $\xi_x = \partial\xi/\partial x$ etc.); $J = \xi_x\psi_y\zeta_z + \xi_y\psi_z\zeta_x + \xi_z\psi_x\zeta_y - \xi_z\psi_y\zeta_x - \xi_y\psi_x\zeta_z - \xi_x\psi_z\zeta_y$ is Jacobian for the exchange of the two coordinates. $P = p/\rho_0$, p is the air pressure, ρ_0 is the air density, and τ_{ij} ($i, j = 1, 2, 3$) is the trace-free subgrid-scale Reynolds stress. The Smagorinsky-type subgrid scheme (1963) was used in our model considering the balance between shear production and dissipation by the topography and the windbreak. Thus, we have subgrid-scale Reynolds stress in the generalized terrain-following coordinates (ξ, ψ, ζ) as follows:

$$\begin{aligned} \tau_{ij} &= \nu \cdot D_{ij} \\ D_{ij} &= \xi_j \cdot \frac{\partial u_i}{\partial \xi} + \psi_j \cdot \frac{\partial u_i}{\partial \psi} + \zeta_j \cdot \frac{\partial u_i}{\partial \zeta} + \xi_i \cdot \frac{\partial u_j}{\partial \xi} + \psi_i \cdot \frac{\partial u_j}{\partial \psi} + \zeta_i \cdot \frac{\partial u_j}{\partial \zeta} \\ \nu &= (C_s \Delta)^2 \left(0.5 \sum_{i,j=1}^3 D_{ij}^2 \right)^{1/2} \\ \Delta^3 &= \Delta x \Delta y \Delta z = \frac{\Delta \xi \Delta \eta \Delta \zeta}{J} \\ C_s &= 0.12 \end{aligned} \quad (3)$$

where C_s is called the Smagorinsky constant. At the surface boundary we assume that neutral stratification can be applied to the ζ axis. The boundary conditions are defined as follows:

- (a) at the ground surface: $u = v = w = 0, \partial P/\partial \zeta = 0$,
- (b) at the top of the domain: $\partial u/\partial \zeta = \partial v/\partial \zeta = \partial w/\partial \zeta = \partial P/\partial \zeta = 0$,
- (c) at the inflow boundary: $u = u_0, v = v_0, w = w_0, \partial P/\partial n = 0$,
- (d) at the outflow boundary: $\partial u/\partial n = \partial v/\partial n = \partial w/\partial n = \partial P/\partial \zeta = 0, n = \xi, \psi, \zeta$.

Details about the transformation of coordinates, parameterization, grid formation and numerical aspects of the model are given in Du *et al.* (1997).

Simulation description

Two cases were considered using the model. One uses a 2-m-high windbreak hedge for preventing wind erosion around a barchan sand dune which is 5 m high, 64 m wide and 96 m long. Simulations of the windbreak effects on airflow distributions were carried out by erecting 2-m-high windbreak hedges at different places over and around the sand dune. As shown in Fig. 1, the horizontal grids were 80 * 80 by 2 m

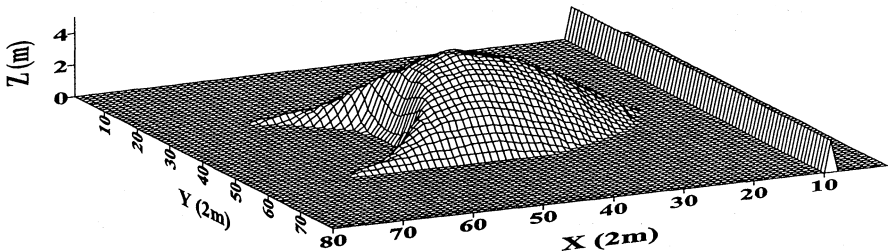


Fig. 1 Sand dune, windbreak and grid system used in the simulation.

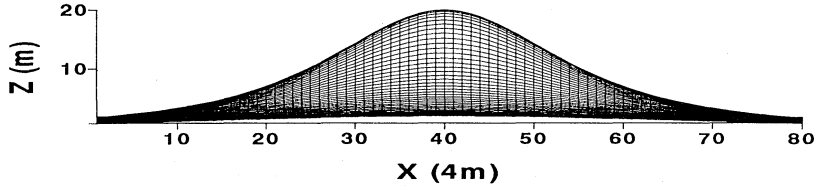


Fig. 2 Profile of an idealized hill used in the simulation.

intervals as indicated by X and Y . The vertical levels were 10 (including the surface level) and the upper limit of the domain was 18 m for quick calculation. The windbreak was a 2-m-high hedge with 0% porosity. As shown in Fig. 1, the hedge was 2 m wide at the base and tapered to a point at the top. The 2-m hedge was placed in three different positions to simulate the windbreak effects on airflow over the sand dune: 18 m upwind of the dune ($x = 9$), directly in front of the dune ($x = 18$) and 18 m upwind of the summit of the dune ($x = 32$) respectively. Another case is simulating the effect of terrace and windbreak hedge construction on an idealized hill 20 m high and 320 m wide. As shown in Fig. 2, the horizontal grids were $80 * 80$ by 4 m interval as indicated by the letters X and Y . The vertical levels were 20 (including surface level) and the upper limit of the domain was 38 m for quick calculation. The hill was reshaped by constructed seven terraces at 1 m, 3 m, 5 m, 7 m, 10 m, 14 m and 18 m as shown in Fig. 3. The effect of the terrace construction on wind distribution was simulated. Furthermore, 2-m-high windbreak hedges were erected at the edges of each terrace except on the 1-m terrace and the effect on wind distribution was simulated.

The initial wind was 5.0 m s^{-1} to the dune, hill, dune with hedge, hill with terrace and hill with terrace and hedge. That is $u_0 = 5.0 \text{ m s}^{-1}$, $v_0 = w_0 = 0.0$. The time interval was 0.1 s. The results of 2000 steps or after 3 min 20 s, when the stationary effect of the flow field was obtained, were used for the evaluation. Only the horizontal wind component in the main direction (i.e. the u component) at 1.5 m above the ground are discussed in this paper.

SIMULATION RESULTS

Case one: sand dune and windbreak

Figure 4 shows the horizontal distribution of wind speed 1.5 m above ground surface over and around the dune for four conditions: (a) without hedge and (b)–(d) with a

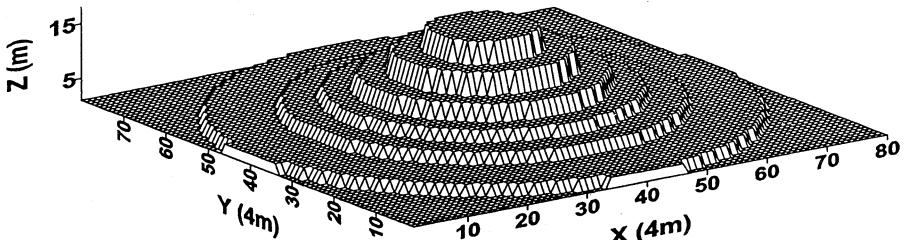


Fig. 3 Terrace construction on the hill and grid system used in the simulation.

2-m hedge in three different places. As shown in Fig. 4, there was a speedup region on the windward side of the barchan sand dune and a reduction region in the leeward side of the dune. Wind was strongest on the windward side of the dune summit and grew weaker once it had passed the summit. It was also weak on both wings of the leeward slope of the dune. It can therefore be conjectured that when the wind gains in strength, the dune will move or roll downwind retaining its barchan shape. Comparing Fig. 4 (a) to Fig. 4 (b)–(d), it can be seen that the overspeeding area in the windward side, which existed when there is no windbreak, disappeared when the hedge was erected 18 m windward of the summit of the dune. The area of wind speed over 2.0 m s^{-1} was only on the windbreak hedge while that was about a third of the area occupied by the windward side of the dune. However, due to the integrated effect of topography and windbreak, airflow around and over the sand dune did not change substantially when the hedge was placed directly in front of the dune. Wind reduction was smallest due to overspeeding of the sand dune. When the windbreak hedge was set up 18 m windward of the dune, there was no influence on the airflow

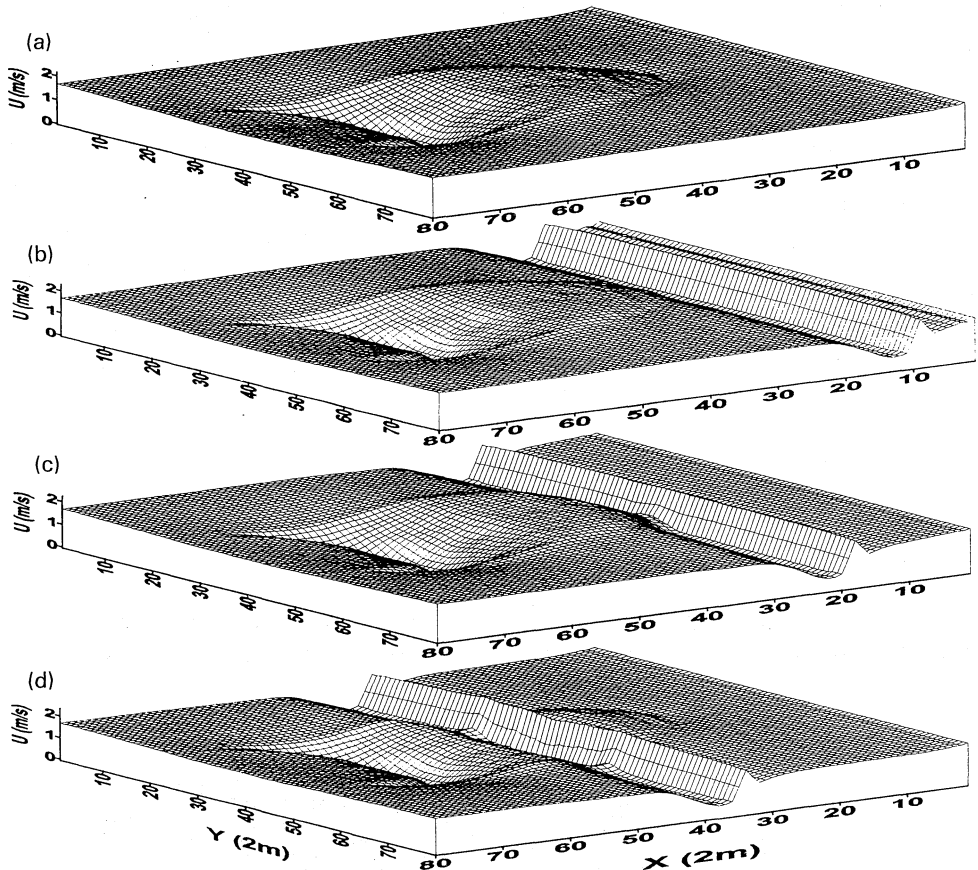


Fig. 4 Horizontal distributions of wind speed 1.5 m above ground surface over and around the dune without a windbreak (a) and with 2 m hedge placed in three different places: 18 m upwind of the dune ($x = 9$) (b), directly in front of the dune ($x = 18$) (c) and 18 m upwind of the summit of the dune ($x = 32$) (d), respectively.

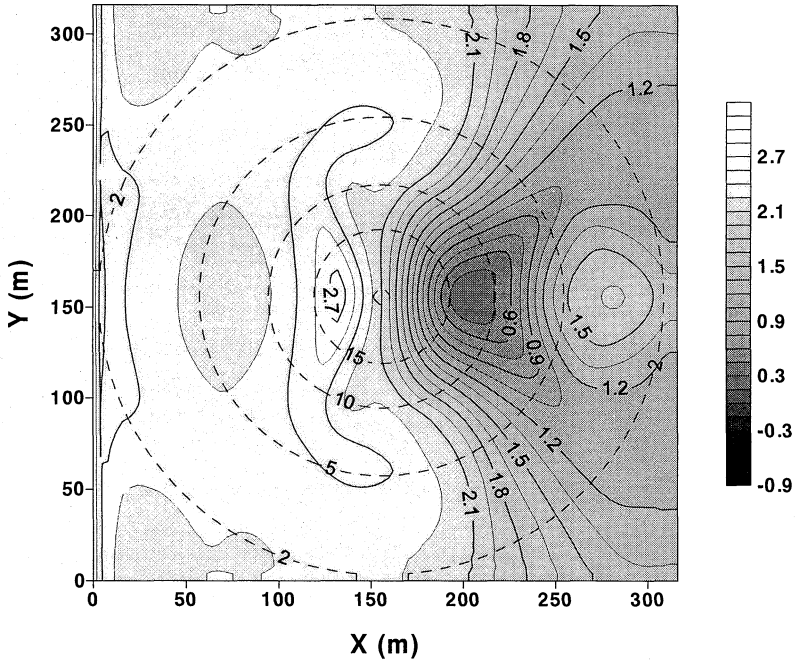


Fig. 5 Horizontal distribution of simulated wind speed 1.5 m above the ground over a 20-m-high idealized hill (dish lines indicate the contour of the hill).

over the sand dune since a 2-m-high hedge only reduced wind speed from 10 m windward to 20 m leeward of the break. When the windbreak hedge was set up 18 m windward of the summit of the dune, the reduction of wind speed was about twice that of when the hedge was located directly in front of the dune. Therefore, the most effective position would be about 18–22 m in front of the summit of the dune.

Case two: hill, terrace and windbreak

Figure 5 shows the horizontal distribution of simulated wind speed (u component) 1.5 m above the ground over the 20-m-high idealized hill. Firstly, it can be seen that the wind was stronger on the windward side ($X < 160$) than on the leeward side ($X > 160$). Then, it is clear that there was a speedup region at the upper part of the windward slope and the middle part of the two side slopes, and there was a region of reduction at the middle part of the leeward slope. The wind was strongest near the top of the hill on the windward side and then the wind became weaker and weaker until the middle part of the leeward slope. This result is in good agreement with observation data (e.g. Fu, 1981). As shown in Fig. 6, when seven terraces (1 m, 3 m, 5 m, 7 m, 10 m, 14 m and 18 m) were constructed (dish lines indicate the edge of the terraces) the wind speed distribution pattern changed greatly. Although the 4 * 4-m grid system was sparse for the 2–4-m-high terraces, it is clear that the wind speed was reduced on the terraces except in the middle part of the leeward slope of the hill. There was a noticeable wind speed reduction on the windward side resulting

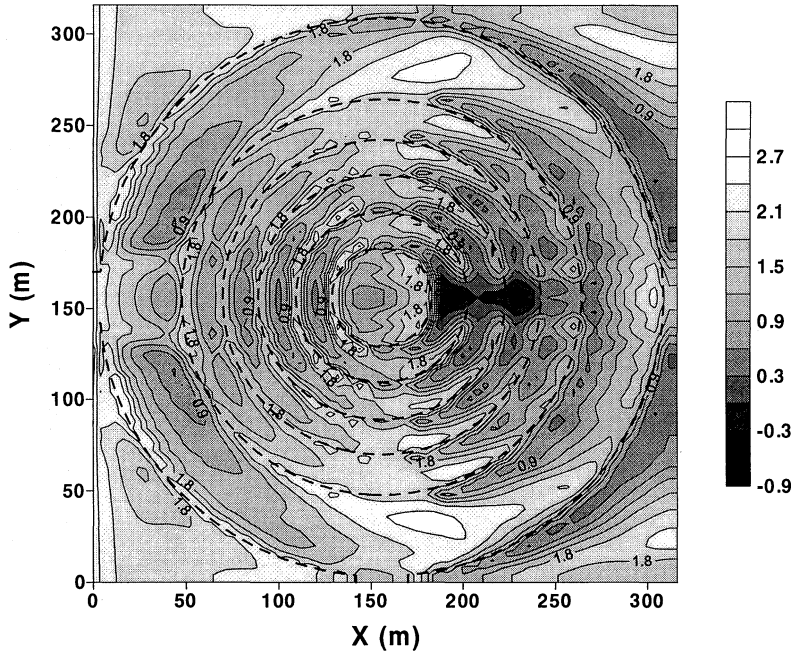


Fig. 6 Horizontal distribution of wind speed 1.5 m above the ground over the hill with seven terraces (dish lines indicate the terrace edges at: 3 m, 5 m, 7 m, 10 m, 14 m and 18 m).

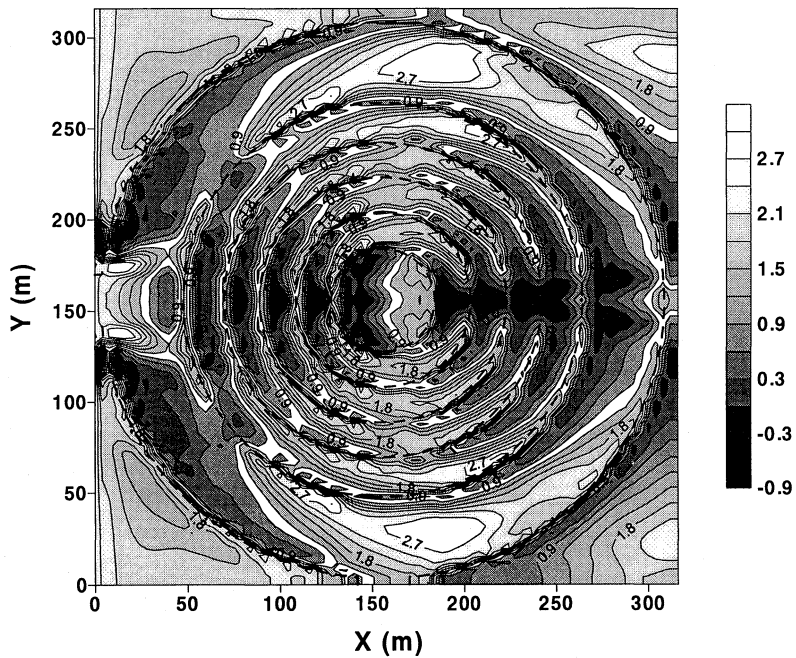


Fig. 7 Horizontal distribution of wind speed 1.5 m above the ground over a 20-m-high idealized hill with seven terraces and 2-m high windbreaks at the edges of the terraces (dish lines indicate the edge of the terraces with 2-m high hedge: 5 m, 7 m, 9 m, 12 m, 16 m and 20 m).

in the disappearance of the speedup region at the upper part of the windward slope (cf. Fig. 5). The wind was relatively strong in the centre section (around $X = 160$) between the windward and the leeward side. Comparing Fig. 6 to Fig. 5, it is evident that wind reduction was over 40% in most places on the hill. If 2-m-high windbreak hedges were constructed at the edges of each terrace except on the 1-m terrace, the simulated wind speed would reduce further on each terrace as shown in Fig. 7. The simulated wind distribution patterns did not change much compared to Fig. 6. However, the wind speed was reduced about 20–40% in most places and was increased about 20% at the lower part of two side slopes where the strongest wind existed. Therefore, it can be concluded that terrace construction on a hill could change the wind distribution and reduce wind speed on terraces especially on the windward side. Construction of windbreaks at the edge of terraces could further reduce wind speed on terraces. However, wind speed would increase at the lower part of two side slopes of the hill. It is necessary to built windbreaks on the terraces orthogonalized to terrace edges to prevent this region appearing.

Acknowledgement This study was supported by grants from the Ministry of Agriculture, Forestry and Fisheries, Japan.

REFERENCES

- Du, M. & Maki, T. (1993) A preliminary study on the prevention of drifting sands and desertification in arid areas. *J. Agric. Met.* **48**, 687–690.
- Du, M. & Maki, T. (1997) Effect of polyethylene windbreak nets on drifting sand and microclimate. *J. Agric. Met.* **52**, 953–956.
- Du, M., Wu, P., Maki, T. & Kawashima, S. (1997) A three dimensional numerical model of the flow over a complex terrain with height variation less than 100 m. In: *Proceedings of MODSIM97* (ed. by McDonald & McAleer) (Proc. Int. Congress on Modelling and Simulation, Hobart, Australia, December 1997). The Modelling and Simulation Soc. of Australia Inc.
- Fisher, P. F. & Galdies, P. (1988) A computer model for barchan-dune movement. *Computer & Geosci.* **14**(2), 229–253.
- Fu, B. (1981) *Microclimate and Local Climate* (in Chinese). Text Book of Najing University, Najing, China.
- Heisler, G. M., & DeWalle, D. R. (1988) Effects of windbreak structure on wind flow. *Agric. Ecosyst. Environ.* **22/23**, 41–69.
- Judd, M. J., Raupach, M. R. & Finnigan, J. J. (1996) A wind tunnel study of turbulent flow around single and multiple wind breaks. Part 1: Velocity fields. *Boundary-Layer Met.* **80**, 127–165.
- Maki, T. (1982) Studies on the windbreak nets. 4: Characteristics of wind speed profiles near various windbreak nets obtained by wind tunnel experiments (in Japanese with English abstract). *J. Agric. Met.* **38**, 123–133.
- Maki, T., Pan, B., Du, M. & Samejima, R. (1995) Effects of forest and net windbreaks on climatic improvement and protection of sand movement in arid lands of northwestern China. *J. Arid Land Studies* **5**(S), 107–110.
- Maki, T., Du, M., Samejima, R. & Pan, B. (1997) Movement of sand dune in Xinjiang of northwest China and prevention of desertification by windbreak facilities in arid China. *J. Agric. Met.* **52**, 633–636.
- McNaughton, K. G. (1988) Effects of windbreaks on turbulent transport and microclimate. *Agric. Ecosyst. Environ.* **22/23**, 17–39.
- Smagorinsky, J. (1963) General circulation experiments with the primitive equations. I. The basic experiments. *Mon. Weath. Rev.* **91**, 99–164.
- Van Eimern, J., Karschon, R., Razumova, L. A. & Robertson, G. W. (1964) Windbreaks and shelterbelts. *WMO Tech. Note no. 59, Geneva, Switzerland.*
- Wang, H. & Tatle, E. S. (1995) A numerical simulation of boundary-layer flow near shelterbelts. *Boundary-Layer Met.* **75**, 141–173.
- Wilson, J. D. (1985) Numerical studies of flow through a windbreak. *J. Wind Eng. Ind. Aerodyn.* **21**, 119–154.
- Wippermann, F. K. & Gross, G. (1986) The wind-induced shaping and migration of an isolated dune: a numerical experiment. *Boundary-Layer Meteorol.* **36**, 319–334.